

## Short Article

# Different vertical distribution of diatoms in sea ice at the river mouth and off the eastern coast of Saroma-ko Lagoon, Hokkaido, Japan

Keigo D. Takahashi<sup>1,2\*,3\*</sup>, Daiki Nomura<sup>2,4,5</sup>, Yuichi Nosaka<sup>6</sup>

**Abstract:** The composition and cell abundance of diatoms in sea ice near the eastern coast of Saroma-ko Lagoon, Hokkaido, Japan, and near the mouth of the Saromabetsu River were reported in late February and early March 2023. Off the lagoon coast, a diatom bloom ( $13.6 \times 10^6$  cells  $l^{-1}$ ) dominated by *Detonula confervacea* was found at the bottom 5 cm of sea ice. At the river mouth, however, the diatom cell abundance was highest in the top 5–10 cm layer ( $9.9 \times 10^6$  cells  $l^{-1}$ ) and decreased with the depth of the sea ice. The diatom community here was overwhelmingly dominated by arborescent colonies of marine diatom *Nitzschia frigida* throughout the ice ( $4.4 \times 10^5$ – $9.9 \times 10^6$  cells  $l^{-1}$ ), accounting for 97–100% of the total cells, which were thought to be adapted to the bottom ice environment. The high cell abundance at the river mouth was associated with lower nutrient concentrations implying that *N. frigida* had consumed nutrients of river water trapped in sea ice. These results suggest that the composition and vertical distribution of diatom species in sea ice in the lagoon can differ at a small spatial scale.

**Key words:** Fast ice; Ice algae; Ice algal bloom; *Nitzschia frigida*; *Detonula confervacea*

## Introduction

Saroma-ko Lagoon (Hokkaido, Japan) is the lowest-latitude area covered by sea ice in the Northern

Hemisphere. From January to March, sea ice covers on average > 60% of the lagoon (Tateyama and Enomoto, 2011) and ice thickness can exceed 50 cm (Nomura et al., 2022). Sea ice algae are the major primary

<sup>1</sup> Graduate University for Advanced Studies, SOKENDAI, 10-3 Midori-cho, Tachikawa, Tokyo 190-8518, Japan.

<sup>2</sup> Field Science Center for Northern Biosphere, Hokkaido University, Hakodate, Hokkaido 041-8611, Japan.

<sup>3</sup> Japan Society for the Promotion of Science Research Fellow, 5-3-1, Kōjimachi, Chiyoda-ku, Tokyo 102-0083, Japan

<sup>4</sup> Faculty of Fisheries Science, Hokkaido University, 3-1-1, Minato-cho, Hakodate, Hokkaido 041-8611, Japan.

<sup>5</sup> Arctic Research Center, Hokkaido University, Kita-21 Nishi-11, Kita-ku, Sapporo 001-0021, Japan.

<sup>6</sup> Department of Marine Biology and Sciences, School of Biological Sciences, Tokai University, 5-1-1, Minamisawa, Minami-ku, Sapporo, Hokkaido 005-0825, Japan.

\* Corresponding Author

受付日：2024年7月5日，受理日：2024年12月3日，WEB掲載日：2024年12月31日

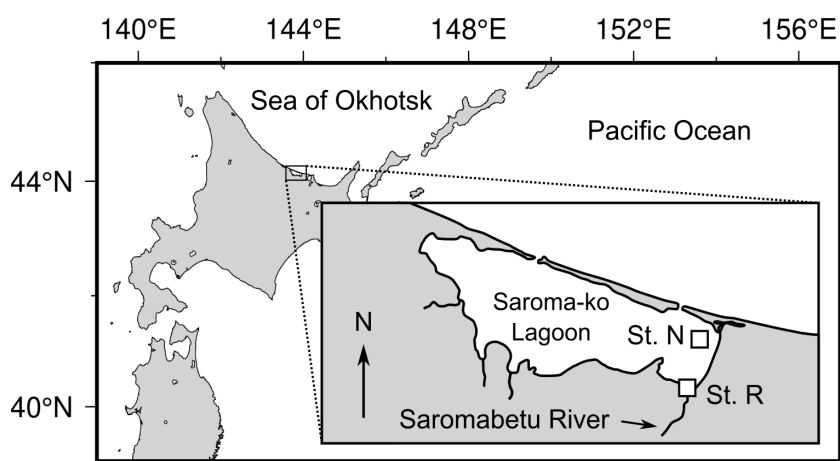


**Fig. 1** Sampling locations in Saroma-ko Lagoon, Hokkaido, Japan.

producers, and their productivity is equivalent to that in the water column (Satoh et al., 1989). They develop high concentrations compared to the underlying phytoplankton, and chlorophyll *a* (Chl *a*) concentrations can reach  $> 290 \mu\text{g l}^{-1}$  in the bottom 10 cm of the ice layer (Nomura et al., 2022). During ice-melting periods, ice algae are released from the sea ice, and some can occasionally trigger phytoplankton blooms in seawater (Wilson et al., 1986) by acclimating to the seawater environment (e.g., higher light and low salinity). The remaining algal cells sink to the depths, providing organic matter for zooplankton (Saito and Hattori, 1997), or are subject to sedimentation at the water bottom (Sakoh et al., 1997; Taguchi et al., 1997).

To understand the role of sea ice in the primary production in seasonally ice-covered oceans, it is necessary to obtain information on the species composition and cell abundance of ice algae. In Saroma-ko Lagoon, various microalgae have been reported from sea ice (Ikeya et al., 2001; Yoshida et al., 2020; Nomura et al., 2024). The large pool size of photoprotective pigments and high plasticity in photosynthetic performance relative to light availability suggest that ice-algal communities can respond to fluctuating and low-light conditions (Aikawa et al., 2009; Takimoto et al., 2017; Yoshida et al., 2020). Their photosynthetic performance, however, depends on the species, based on studies in Saroma-ko Lagoon (Takimoto et al., 2017) and other oceanic water bodies (Yoshida et al., 2018;

Takao et al., 2020). In addition to photosynthesis in sea ice, subsequent bloom formation in seawater may depend on the species composition of ice algae, because a limited number of species form blooms after sea ice melts (Takahashi et al., 2022). Understanding the spatial and temporal variability of ice-algal compositions can therefore help to elucidate the impact of sea ice on primary production in seasonal ice zones.

In this study, we focused on the diatom communities at two sites in Saroma-ko Lagoon, one of which is close to the river mouth and feeds into the lagoon. Previous floristic studies sampled sea ice in the inner areas of Saroma-ko Lagoon, which was likely formed via the freezing of seawater (salinity  $\sim 32$ , Nomura et al., 2022) and focused on the most productive bottom community (Yoshida et al., 2020). The diatoms *Detonula confervacea*, *Odontella* sp., *Navicula* spp. and *Fragilariopsis cylindrus* are commonly found and dominant in sea ice (Taguchi et al., 1995; Ikeya et al., 2001; Takimoto et al. 2017; Yoshida et al., 2020; Nomura et al., 2022, 2024). However, four major rivers enter the lagoon, providing freshwater to the system (Fig. 1). Brackish water at river mouths may lead to biota that differ from those in the offshore areas. Possible reasons for this include the input of freshwater or brackish species during sea ice formation and differences in nutrient concentrations and salinity. Hence, we report for the first time the cell abundance and species composition of ice algae at the mouth of the Saromabetu River.

## Materials and methods

The observation was conducted in Saroma-ko Lagoon in northern Japan at St. N (44°07'12" N, 143°57'21" E) on February 28, 2023 and at St. R (44°04'48" N, 143°56'12" E) on March 1, 2023 (Fig. 1) as part of a multidisciplinary study on sea ice (Nomura et al., 2024). The distance between the two stations was approximately 4.7 km. The water depth was 6.0 m at St. N and 1.8 m at St. R. A set of two sea ice cores (one for salinity, Chl *a*, and nutrient concentration and the other for microscopic analysis) was collected at each station using a standard corer (90 mm diameter, Mark II coring system; Kovacs Enterprises, Inc.). The ice thicknesses were 35 cm and 45 cm at St. N and St. R, respectively for the measurements of salinity, Chl *a*, and nutrient concentration measurements (Nomura et al., 2024). Those for microscopic analysis were 36 cm (St. N) and 45 cm thick (St. R). At St. N, ice cores were cut into six and seven sections (5–7 cm thickness per each section) for microscopy and the other parameters, respectively. At St. R, they were cut into nine sections with uniform thickness (5 cm) for all parameters.

For the microscopic analysis, each ice section was allowed to melt at room temperature without adding filtered seawater. Algal cells in sea-ice meltwater were fixed by adding neutral Lugol's iodine solution (Edler and Elbrächter, 2010, final concentration 2%) and stored at +4°C in the dark. At least 400 cells were counted using an inverted light microscope ( $\times 400$  magnification) after concentrating 10 ml of water in an Utermöhl chamber (Edler and Elbrächter, 2010). Only the cells with protoplasts were counted for calculating cell abundance (cells l<sup>-1</sup>). Sea-ice salinity, Chl *a*, and macronutrient (NO<sub>3</sub><sup>-</sup>, PO<sub>4</sub><sup>3-</sup>, and Si(OH)<sub>4</sub>) concentrations were obtained from Nomura et al. (2024). Under-ice water (+1 m and +0.6 m from the ice bottom at St. N and St. R, respectively) and slush (snow mixed with seawater at the top of sea ice) were also collected for salinity and macronutrient measurements (Nomura et al., 2024). To identify the *Navicula* species in the top and bottom ice samples, diatom valves were observed at  $\times 1,000$  magnification under an upright light microscope. Diatom valves were cleaned (removing protoplast) by a bleaching agent (Nagumo, 1995) and the permanent slides were prepared following Takahashi and Makabe (2023).

The relationships between total cell abundance and

nutrient concentrations were plotted after normalizing the nutrient concentration to the salinity of under-ice water and sea ice. Because macronutrient concentration is highly dependent on sea ice salinity, its relationship with algal concentration can be obscured by physical changes in sea ice such as the release (decrease) of nutrients by the desalination of sea ice (Fripiat et al., 2017). Therefore, we determined the salinity-normalized nutrient concentration (Fripiat et al., 2017), which is calculated as follows:

$$*C = \frac{S_w}{S_i} \times C$$

where \*C is the salinity-normalized concentration; S<sub>w</sub> and S<sub>i</sub> are the salinities of under-ice water and sea ice, respectively; C is the bulk concentration of sea ice (NO<sub>3</sub><sup>-</sup>, PO<sub>4</sub><sup>3-</sup>, and Si(OH)<sub>4</sub>). S<sub>w</sub> was 27.6 at St. N and 0.6 at St. R.

## Results

The total diatom cell abundance in sea ice ranged from 4.4  $\times 10^5$  cells l<sup>-1</sup> to 13.6  $\times 10^6$  cells l<sup>-1</sup> (Fig. 2). The maximum diatom cell abundance was found in the bottom 31–36 cm layer at St. N, and in the top 5–10 cm layer at St. R (Fig. 2). Chl *a* concentration ranged from 3.2–71.2  $\mu\text{g l}^{-1}$  and corresponded with the diatom distribution.

Microscopic analysis using an Utermöhl chamber identified 10 and 3 genera at St. N and St. R, respectively. Four taxa among them were identified only at the genus level. The species composition was also different between the two stations, where diverse communities (*Detonula confervacea*, *Melosira arctica*, and *Chaetoceros* spp.) were found at St. N, while arborescent colonies of the marine diatom *Nitzschia frigida* (Fig. 3f) accounted for 97.1–100.0% of the total cells throughout the sea ice core at St. R. At St. N, *D. confervacea* was predominant in the sample from the ice bottom (83.3%). In contrast, its contribution to the total cells gradually decreased towards the upper layers. The top and middle layers of sea ice had higher contributions of *Chaetoceros* spp. (0.0–17.3%), *Fragilariopsis* spp. (1.8–14.2%), and *Navicula* spp. (0.4–13.9%). According to the observations of the cleaned materials, the identified *Navicula* species included *N. transitans* and *N. septentrionalis* at St. N and *N. lanceolata* at St. R. Of the identified diatoms, both

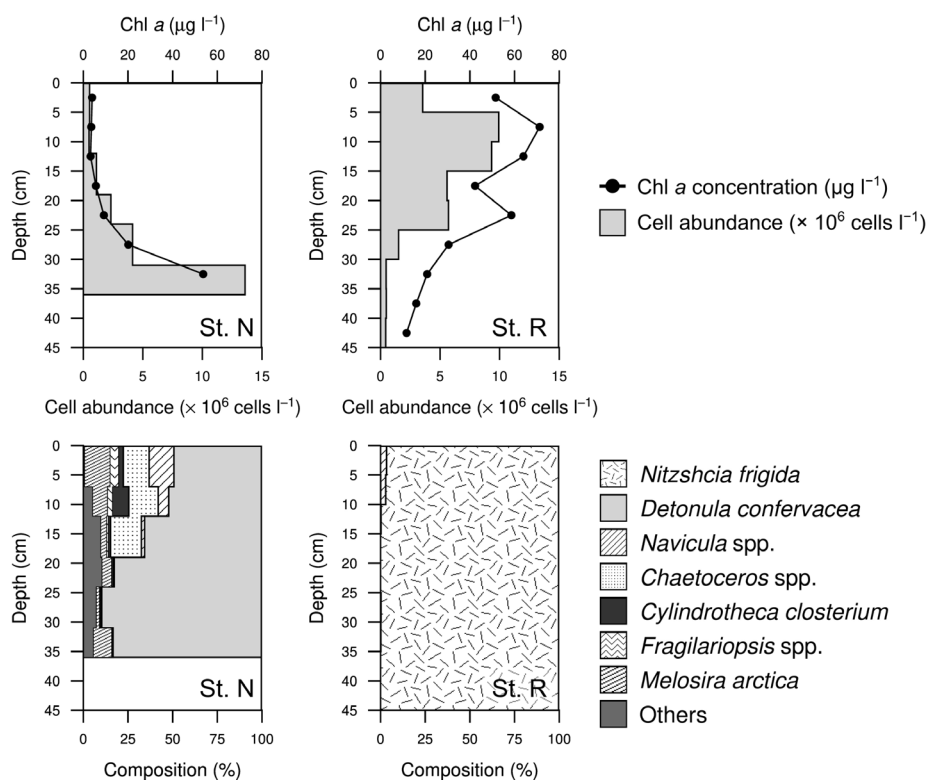


**Fig. 2** Vertical distribution of chlorophyll *a* concentration, total cell abundance and species composition of diatoms.

fresh (*Navicula lanceolata*) and marine diatoms (others) were detected at St. R.

Sea ice salinity was significantly lower at St. R (0.0–2.0) than at St. N (3.6–10.5) and highest at 0–5 cm layers (Fig. 4a–c). The bulk macronutrient concentration generally increased with higher salinity and except  $\text{NO}_3^-$  at St. N and the maximum concentration was found in slush (0 m) at both stations.  $\text{NO}_3^-$ ,  $\text{PO}_4^{3-}$ , and  $\text{Si}(\text{OH})_4$  concentrations ranged 1.3–9.6  $\mu\text{mol l}^{-1}$ , 0.2–1.3  $\mu\text{mol l}^{-1}$ , 5.2–32.9  $\mu\text{mol l}^{-1}$ , respectively at St. N, being generally lower than St. R (4.2–52.5  $\mu\text{mol l}^{-1}$ , 0.6–4.2  $\mu\text{mol l}^{-1}$ , 1.5–138.9  $\mu\text{mol l}^{-1}$ , for  $\text{NO}_3^-$ ,  $\text{PO}_4^{3-}$ , and  $\text{Si}(\text{OH})_4$ , respectively).

The salinity-normalized nutrient concentrations ( $^*\text{NO}_3^-$ ,  $^*\text{PO}_4^{3-}$ , and  $^*\text{Si}(\text{OH})_4$ ) showed different trends at St. N and St. R (Fig. 4d–i). At St. N, nutrient concentration generally increased with diatom total cell abundance but only  $^*\text{Si}(\text{OH})_4$  had significant linear relationship (Pearson correlation coefficient,  $r = 0.90$ ,  $p < 0.05$ , Fig. 4f). At St. R,  $^*\text{NO}_3^-$  and  $^*\text{Si}(\text{OH})_4$  decreased with higher cell abundance and the relationship with  $^*\text{NO}_3^-$  was found significant (Pearson correlation coefficient,  $r = -0.73$ ,  $p < 0.05$ , Fig. 4g).

## Discussion

The vertical distribution of Chl *a* concentration at St. N agrees with previous studies, where sea-ice algae develop at the bottom part (~10 cm from the bottom), and Chl *a* concentration in this layer reaches  $> 290 \mu\text{g l}^{-1}$  (Nomura et al., 2022). However, algal blooms in the top layer of the sea ice (St. R) have rarely been reported in fast ice (Whitaker and Richardson, 1980). In first-year or multiyear ice, macronutrients are scarce in the upper part of the sea ice unless there is flooding or flushing of seawater (Whitaker and Richardson, 1980) or vertical convection of brine (Fritsen et al., 1994) or snowfall (Nomura et al., 2011). According to Nomura et al. (2024),  $\text{NO}_3^-$ ,  $\text{PO}_4^{3-}$ , and  $\text{Si}(\text{OH})_4$  concentrations were higher at the top (snow-ice interface) and bottom of the sea ice at both stations, suggesting that both snow and seawater provided nutrients (Nomura et al., 2011). In this study, the bulk concentrations of  $\text{NO}_3^-$ ,  $\text{PO}_4^{3-}$ , and  $\text{Si}(\text{OH})_4$  were generally higher at the upper sea ice layers, corresponding to sea ice salinity (Fig. 4a–c). The release and convection of brine at the lower layers (Tison et al.,

Different vertical distribution of diatoms in sea ice at the river mouth  
and off the eastern coast of Saroma-ko Lagoon, Hokkaido, Japan

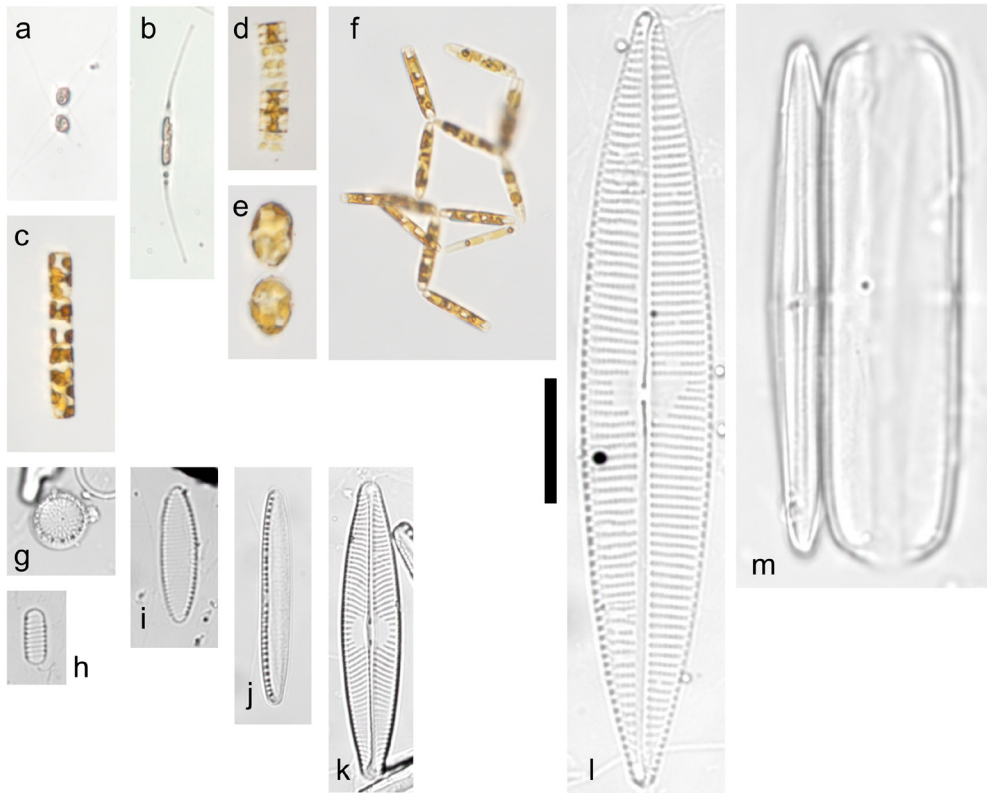


**Fig. 3** The dominant diatom species found in sea ice. The Lugol-fixed cells (a–f) and the cleaned materials (g–m) prepared following Nagumo (1995) and Takahashi and Makabe (2023). a: *Chaetoceros* sp., b: *Cylindrotheca closterium*, c: *Detonula confervacea*, d: *Fragilariopsis* sp., e: *Melosira arctica*, f: *Nitzschia frigida*, g: *Detonula confervacea*, h: *Fragilariopsis cylindrus*, i: *Fragilariopsis oceanica*, j: *Nitzschia frigida*. k: *Navicula lanceolata*, l: *Navicula transitans*, and m: *Navicula septentrionalis* (valve and girdle views). The scale bar is 50  $\mu\text{m}$  for images a–f and 20  $\mu\text{m}$  for images g–m. The figures a–e, g–i, and l, m are from St. N and figures f, j, k are from St. R.

2008) or flooding of seawater at the top by tide (Ishii and Toyota, 2012) or input from snow (Nomura et al., 2011) likely influenced the vertical distribution of salinity and nutrients. However, the average concentrations of the three macronutrients in sea ice were 2.4–3.3 times higher at St. R than at St. N (Fig. 4a–c). At St. R, ice salinity and temperature showed little vertical fluctuation (ranging from 0.5 to 2.0 for salinity and  $-0.1$  to  $+0.1^\circ\text{C}$  for temperature), suggesting that brine convection and nutrient replenishment following the cooling of ice (Fritsen et al., 1994) was not responsible for the high nutrient concentration at St. R. Macronutrient concentrations in snow at St. R were only 0.0–0.7 times of those at St. N (Nomura et al., 2024), therefore snowfall does not explain higher nutrient availability at St. R. The

macronutrient concentration of under-ice water (i.e., the origin of sea ice) was 4.5–11.7 times higher at St. R than St. N which is shown as the steeper theoretical dilution lines (Fig. 4a–c). This likely led to higher bulk nutrient concentrations in sea ice at St. R, particularly in the high saline upper layers, supporting the development of algae in the ice.

The relationships between diatoms and nutrient concentration differed between the two stations;  $^*\text{Si}(\text{OH})_4$  was enriched with increased total cell abundance at St. N while  $^*\text{NO}_3^-$  was negatively correlated with cell abundance (Fig. 4f, g). This is likely due to the vertical distribution of ice algae. St. N and previous studies have found algal concentration is highest in the bottom of the sea ice, where nutrients are more available from

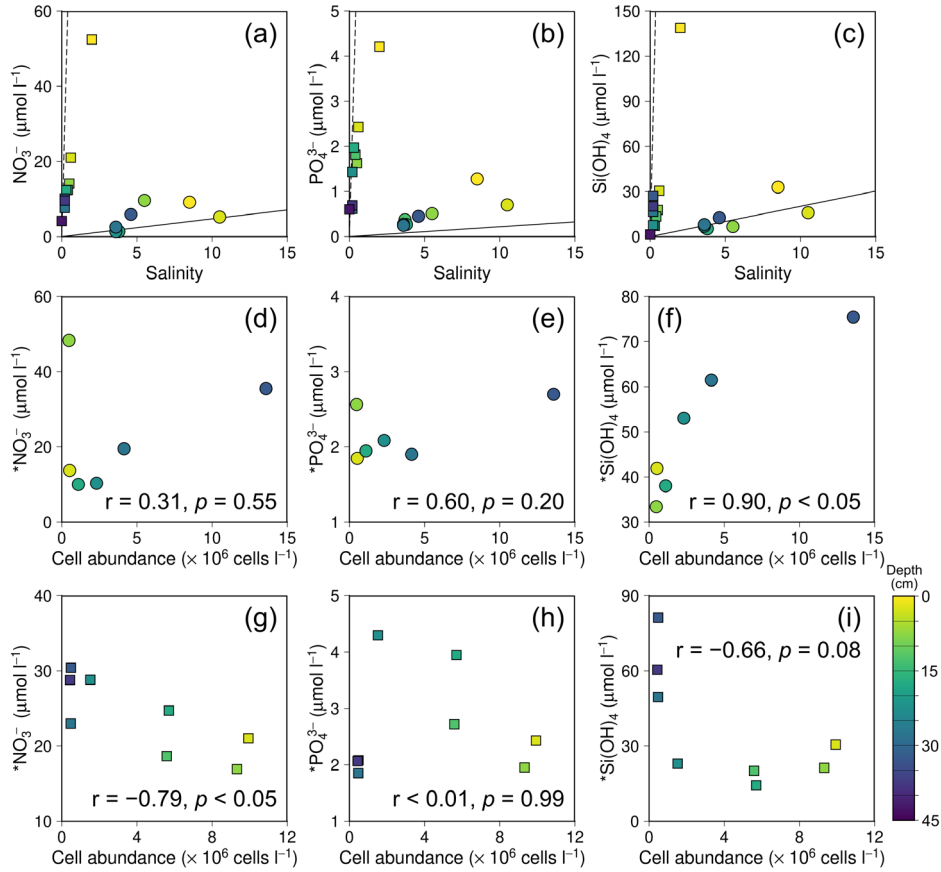


**Fig. 4** Salinity and macronutrient concentration in sea ice and slush (a–c) from Nomura et al. (2024). The circles and squares represent St. N and St. R, respectively. The theoretical dilution lines (TDL) are plotted using under-ice water salinity and nutrient concentration data of under-ice water. The solid and dashed TDL represent St. N and St. R respectively. The relationships between total cell abundance and salinity-normalized nutrient concentrations at St. N (d–f) and St. R (g–i). The coefficients ( $r$ ) and  $p$ -values are from Pearson correlation.

seawater (Taguchi et al., 1995; Wongpan et al., 2020). Ishii and Toyota (2012) found brine salinity at the bottom of sea ice was higher than the under-ice seawater off the eastern coast during the mid-February. This condition enhances vertical convection of brine and seawater and could introduce nutrients into sea ice (Tison et al., 2008). At St. R, algal bloom developed in the interior of sea ice, being remote from the sources of nutrient (seawater). In contrast, \*PO<sub>4</sub><sup>3-</sup> showed no relationship both at St. N and St. R (Fig. 4e, h). PO<sub>4</sub><sup>3-</sup> can be provided by remineralization of phosphorus in organic matter and the enrichment can exceed uptake by algae in sea ice (Fripiat et al., 2017; Takahashi et al., 2022), resulting in the relationship between PO<sub>4</sub><sup>3-</sup> and diatom abundance

indiscernible. These findings suggest that the dominant diatoms *Detonula confervacea* utilized nutrients supplied from under-ice water, while *N. frigida* consumed those from river water trapped in the upper layers.

The diatom composition at St. N agrees with that of previous studies, in which *D. confervacea* dominated off the eastern coast of Saroma-ko Lagoon (Taguchi et al., 1995; Yoshida et al., 2020; Nomura et al., 2022, 2024). It reportedly grows well at moderate temperatures (around 12°C), yet under cold (+2°C) and dim light conditions (< 50 μmol photons m<sup>-2</sup> s<sup>-1</sup>, photosynthetically active radiation, PAR), its division rate surpassed those at higher irradiance (Smayda, 1969). The Chl *a* productivity measured at St. N (Nomura et al., 2024) supports the

notion that this species is adapted to low light (maximum Chl *a* production rate at 29–32  $\mu\text{mol photons m}^{-2} \text{ s}^{-1}$ ). Takimoto et al. (2017) and Wongpan et al. (2020) reported that PAR transmittance of sea ice off the eastern coast of Saroma-ko Lagoon was 0.3–2.5%, which yields 1.0–32.2  $\mu\text{mol photons m}^{-2} \text{ s}^{-1}$  at the bottom. These findings suggest that this species prefers dim light conditions, such as those in the bottom section of sea ice.

The diatom at St. R, *Nitzschia frigida*, is for the first time reported to be dominant in Saroma-ko Lagoon. It has been reported in sediments, sea ice, and seawater in the lagoon but is not dominant (< 5% of the total cell count or algal volume) in sea ice (Taguchi et al., 1995; Ikeya et al., 2001; Satoh et al., 1991). It is deemed as an important primary producer in Arctic sea ice because it occasionally forms blooms in first-year and multiyear ice (up to  $2.5 \times 10^7$  cells  $\text{l}^{-1}$ , von Quillfeldt et al., 2003). This species is known to acclimate to sea ice (high salinity and low temperature) and is expected to survive in under-ice water and be incorporated into ice again from fall to winter (Olsen et al., 2017). Its bloom formation is restricted to the bottom ice or sub-ice layers, where the light intensity is low, and more nutrients are available than in the upper parts of the sea ice (von Quillfeldt et al., 2003). Suzuki and Takahashi (1995) found that it has adapted to cold water (–1.8 to +2.0°C) and low light (maximum growth rate at 50  $\mu\text{mol photons m}^{-2} \text{ s}^{-1}$ ). Croteau et al. (2022) reported even lower light levels for optimal growth (23  $\mu\text{mol photons m}^{-2} \text{ s}^{-1}$ ) at 0°C. In this study, however, the cell abundance of *N. frigida* at St. R was highest near the surface, with a relatively high light intensity. It remains unclear how blooms form in the near-top layer, yet one possibility is that frazil ice may capture phytoplankton during sea ice formation (Garrison et al., 1989). *Nitzschia frigida* was associated with a granular ice layer (sea ice formed via the accretion of frazil ice or snow whose vertical texture appears as a composite of grains) that extends from the top to a depth of 31 cm (Nomura et al., 2024). Satoh et al. (1991) reported *N. frigida* is a benthic diatom in the lagoon, and the shallow water depth at St. R (1.8 m) may support its incorporation from the sediment to sea ice. Frazil ice is reported to contain up to 138.4  $\mu\text{g Chl } a \text{ l}^{-1}$  (DiTullio et al., 1998), and micro-sized *N. frigida* is more efficiently incorporated into frazil ice than smaller (< 4  $\mu\text{m}$ ) algae (Róžańska et al., 2008). Although *Navicula* spp. cells in

this study were similar or larger in size to *N. frigida* cells (Fig. 3k–m); they did not form colonies and present as solitary or doublet cells. Grading and Ikävalko (1998) reported that the larger the cell size, the more efficiently pennate diatoms are incorporated into the newly formed sea ice. The arborescent colonies of *N. frigida* (Fig. 3f) could enhance their incorporation into sea ice. The algal composition and concentration in thinner ice at the earlier season need to be addressed to further test the hypothesis (frazil ice scavenging) on ice algal bloom in the river mouth.

## Conclusion

This study is the first to report algal communities at the river mouth of Saroma-ko Lagoon. Unlike sea ice off the eastern coast, the algal concentration was found peaked in the upper layer of sea ice and was dominated by *N. frigida* which is thought to form blooms in the bottom and sub-ice layers. We found a decrease in  $^*\text{NO}_3^-$  in the *N. frigida*-dominated sea ice, suggesting that *N. frigida* had actively grown in the sea ice resulted in an ice-algal bloom. We surmise that river water rich in macronutrient and shallow water depth (proximity to benthic diatoms including *N. frigida* which are prone to be incorporated during sea ice formation) likely resulted in different vertical distribution and species composition at the two stations in Saroma-ko, Lagoon. Our findings help us understand how brackish water at river mouths can influence ice algal communities as well as biogeochemical properties in sea ice (Nomura et al., 2024).

## Acknowledgements

We would like to express heartfelt thanks to Saroma Research Center of Aquaculture, Napa Kitami, research member for their support in conducting the field work. We thank Dr. Akihiro Shiimoto (Tokyo University of Agriculture) and one anonymous reviewer for their valuable comments which greatly improved the manuscript. This study was supported by the Japan Society for the Promotion of Science (JSPS) KAKENHI Grants Nos. 21J14914 and 24KJ0006 for K.D. Takahashi, and the Arctic Challenge for Sustainability II (ArCS II) (JPMXD1420318865) for D. Nomura.

## References

- Aikawa, S., Hattori, H., Gomi, Y., Watanabe, K., Kudoh, S., Kashino, Y. and Satoh, K. (2009) Diel tuning of photosynthetic systems in ice algae at Saroma-ko Lagoon, Hokkaido, Japan. *Polar Science*, 3 (1): 57–72.
- Croteau, D., Lacour, T., Schiffrine, N., Morin, P. I., Forget, M. H., Bruyant, F., Ferland, J., Lafond, A., Campbell, D.A., Tremblay, J.É., Babin, M. and Lavaud, J. (2022) Shifts in growth light optima among diatom species support their succession during the spring bloom in the Arctic. *Journal of Ecology*, 110 (6): 1356–1375.
- DiTullio, G.R., Garrison, D.L. and Mathot, S. (1998) Dimethylsulfoniopropionate in sea ice algae from the Ross Sea polynya. In: *Antarctic Sea Ice: Biological Processes, Interaction and Variability*, Antarctic Research Series, vol. 73, (eds.) Lizotte, M.P. and Arrigo, K.R. pp. 139–146. American Geophysical Union, Washington D.C.
- Edler, L. and Elbrächter, M. (2010) The Utermöhl method for quantitative phytoplankton analysis. In: *Microscopic and molecular methods for quantitative phytoplankton analysis*, (eds.) Karlson, B., Cusack, C. and Bresnan, E. pp. 13–20. UNESCO, Paris.
- Fripiat, F., Meiners, K.M., Vancoppenolle, M., Papadimitriou, S., Thomas, D.N., Ackley, S.F., Arrigo, K.R., Carnat, G., Cozzi, S., Delille, B., Dieckmann, G.S., Dunbar, R.B., Fransson, A., Kattner, G., Kennedy, H., Lannuzel, D., Munro, D.R., Nomura, D., Rintala, J.-M., Schoemann, V., Stefels, J., Steiner, N. and Tison, J.L. (2017) Macro-nutrient concentrations in Antarctic pack ice: Overall patterns and overlooked processes. *Elementa: Science of the Anthropocene* 5: 13.
- Fritsen, C.H., Lytle, V.I., Ackley, S.F. and Sullivan, C.W. (1994) Autumn bloom of Antarctic pack-ice algae. *Science* 266 (5186): 782–784.
- Garrison, D.L., Close, A.R. and Reimnitz, E. (1989) Algae concentrated by frazil ice: evidence from laboratory experiments and field measurements. *Antarctic Science*, 1 (4): 313–316.
- Gradinger, R. and Ikävalko, J. (1998) Organism incorporation into newly forming Arctic sea ice in the Greenland Sea. *Journal of Plankton Research*, 20 (5): 871–886.
- Ikeya, T., Kikuchi-Kawanobe, K. and Kudoh, S. (2001) Floristic examination of diatom assemblage in the dim light-environment of water column and sea ice, Saroma Ko lagoon, Hokkaido, Japan. *Polar Bioscience*, 14: 33–44.
- Ishii, H. and Toyota, T. (2012) Temporal evolution of the structural properties of seasonal sea ice during the early melt season. *Journal of Glaciology*, 58 (207): 23–37.
- Nagumo, T. (1995) Simple and safe cleaning methods for diatom samples. *Diatom*, 10: 88.
- Nomura, D., McMinn, A., Hattori, H., Aoki, S. and Fukuchi, M. (2011) Incorporation of nitrogen compounds into sea ice from atmospheric deposition. *Marine Chemistry*, 127 (1–4): 90–99.
- Nomura, D., Ikawa, H., Kawaguchi, Y., Kanna, N., Kawakami, T., Nosaka, Y., Umezawa, S., Tozawa, M., Horikawa, T., Sahashi, R., Noshiro, T., Kaba, I., Ozaki, M., Kondo, F., Ono, K., Yabe, I.S., Son, E.Y., Toyoda, T., Kameyama, S., Wang, C., Obata, H., Ooki, A., Ueno, H. and Kasai, A. (2022) Atmosphere-sea ice-ocean interaction study in Saroma-ko Lagoon, Hokkaido, Japan 2021. *Bulletin of Glaciological Research*, 40: 1–17.
- Nomura, D., Akino, R., Corkill, M., Hirano, K., Kasai, A., Katakura, S., Kawaguchi, Y., Kawakami, T., Kimura, R., Lannuzel, D., Makabe, R., Matsuura, M., Matsuno, K., Meiners, K., Nagasaki, K., Nosaka, Y., Samori, N., Sakaya, S., Son, E.Y., Suga, R., Sunakawa, Y., Takahashi, K.D., Takahashi, M., Takeda, Y., Toyota, T., Tozawa, M., Wongpan, P., Yoshida, H., Yoshida, K. and Yoshimura, M. (2024) Multidisciplinary research for sea ice in Saroma-ko Lagoon, Hokkaido, Japan 2023. *Bulletin of Glaciological Research*, 42: 19–37.
- Olsen, L.M., Laney, S.R., Duarte, P., Kauko, H.M., Fernández-Méndez, M., Mundy, C. J., Rösel, A., Meyer, A., Itkin, P., Cohen, L., Peeken, I., Tatarek, A., Róžańska-Pluta, M., Wiktor, J., Taskjelle, T., Pavlov, A.K., Hudson, S.R., Granskog, M.A., Hop, H. and Assmy P. (2017) The seeding of ice algal blooms in Arctic pack ice: The multiyear ice seed repository hypothesis. *Journal of Geophysical Research: Biogeosciences*, 122 (7): 1529–1548.
- Róžańska, M., Poulin, M. and Gosselin, M. (2008) Protist entrapment in newly formed sea ice in the Coastal Arctic Ocean. *Journal of Marine Systems*, 74

- (3–4): 887–901.
- Saito, H. and Hattori, H. (1997) Diel vertical migration and feeding rhythm of copepods under sea ice at Saroma-ko Lagoon. *Journal of Marine Systems*, 11 (1–2): 191–203.
- Sakoh, H., Matsuda, O., Michel, C., Legendre, L., Rajendran, N. and Yamamoto, T. (1997) Temporal variation of chlorophyll-like pigment composition in sinking particles during the ice-covered season in Saroma-ko Lagoon. *Journal of Marine Systems*, 11 (1–2): 123–131.
- Satoh, H., Yamaguchi, Y., Watanabe, K., Tanimura, A., Fukuchi, M. and Aruga, Y. (1989) Photosynthetic nature of ice algae and their contribution to the primary production in Lagoon Saroma Ko, Hokkaido, Japan. *Proceedings of the NIPR Symposium on Polar Biology* 2: 1–8.
- Satoh, H., Yamaguchi, Y., Takeuchi, T. and Watanabe, K. (1991) A comparison of microalgal fatty acids between winter and summer in Lake Saroma, Hokkaido. *Limnology and Oceanography*, 36: 83–89.
- Smayda, T.J. (1969) Experimental observations on the influence of temperature, light, and salinity on cell division of the marine diatom, *Detonula confervacea* (Cleve) Gran. *Journal of Phycology* 5 (2): 150–157.
- Suzuki, Y. and Takahashi, M. (1995) Growth responses of several diatom species isolated from various environments to temperature. *Journal of Phycology*, 31 (6): 880–888.
- Taguchi, S., Demers, S., Fortier, L., Fortier, M., Fujiyoshi, Y., Hattori, H., Kasai, H., M., Kishino, Kudoh, S., Legendre, L., McGinness, F., Mitchel, C., Ngando, T., Robineau, B., Saito, H., Suzuki, Y., Takahashi, M., Therriault, J.-C., Aota, M., Ikeda, M., Ishikawa, M., Takatsuka, T. and Shirasawa, K. (1995) Biological data report for the Saroma-ko site of the SARES (Saroma-Resolute Studies) project, February–March, 1992. *Low Temperature Science, Series A* 53:67–163.
- Taguchi, S., Saito, H., Hattori, H. and Shirasawa, K. (1997) Vertical flux of ice algal cells during the ice melting and breaking periods in Saroma Ko Lagoon, Hokkaido, Japan. *Proceedings of the NIPR Symposium on Polar Biology*, 10: 56–65.
- Takahashi, K.D., Makabe, R., Takao, S., Kashiwase, H. and Moteki, M. (2022) Phytoplankton and ice-algal communities in the seasonal ice zone during January (Southern Ocean, Indian sector). *Journal of Oceanography*, 78 (5): 409–424.
- Takahashi, K.D. and Makabe, R. (2023) Application of the filter-transfer-freeze technique to permanent slide preparation. *Diatom*, 39: 21–24.
- Takao, S., Nakaoka, S. I., Hashihama, F., Shimada, K., Yoshikawa-Inoue, H., Hirawake, T., Kanda, J., Hashida, G. and Suzuki, K. (2020) Effects of phytoplankton community composition and productivity on sea surface  $p\text{CO}_2$  variations in the Southern Ocean. *Deep Sea Research Part I: Oceanographic Research Papers*, 160: 103263.
- Takimoto, K., Katayama, T. and Taguchi, S. (2017) Photoacclimation strategy of ice algal community in the seasonal sea ice. *Plankton and Benthos Research*, 12 (4): 212–223.
- Tateyama, K. and Enomoto, H. (2011) Monitoring freezing condition and its change in the Saroma-ko lagoon by satellite remote sensing. *Journal of Japan Society of Civil Engineers, Ser. B3 (Ocean Engineering)*, 67 (2): I\_727–I\_731.
- Tison, J.L., Worby, A., Delille, B., Brabant, F., Papadimitriou, S., Thomas, D., de Jong, J., Lannuzel, D. and Haas, C. (2008) Temporal evolution of decaying summer first-year sea ice in the Western Weddell Sea, Antarctica. *Deep Sea Research Part II: Topical Studies in Oceanography*, 55 (8–9): 975–987.
- von Quillfeldt, C.H., Ambrose, W.G. Jr. and Clough, L.M. (2003) High number of diatom species in first-year ice from the Chukchi Sea. *Polar Biology*, 26: 806–818.
- Whitaker, T.M. and Richardson, M.G. (1980) Morphology and chemical composition of a natural population of an ice-associated Antarctic diatom *Navicula glaciei*. *Journal of Phycology*, 16 (2): 250–257.
- Wilson, D.L., Smith, W.O. and Nelson, D.M. (1986) Phytoplankton bloom dynamics of the western Ross Sea ice edge—I. Primary productivity and species-specific production. *Deep-Sea Research. Part A. Oceanographic Research Papers*, 33 (10): 1375–1387.
- Wongpan, P., Nomura, D., Toyota, T., Tanikawa, T., Meiners, K. M., Ishino, T., Tamura, T.P., Tozawa, M., Nosaka, Y., Hirawake, T., Ooki, A. and Aoki, S. (2020) Using under-ice hyperspectral transmittance to determine land-fast sea-ice algal biomass in Saroma-

ko Lagoon, Hokkaido, Japan. *Annals of Glaciology*, 61 (83): 454–463.

Yoshida, K., Endo, H., Lawrenz, E., Isada, T., Hooker, S. B., Prášil, O. and Suzuki, K. (2018) Community composition and photophysiology of phytoplankton assemblages in coastal Oyashio waters of the western North Pacific during early spring. *Estuarine, Coastal and Shelf Science*, 212: 80–94.

Yoshida, K., Hattori, H., Toyota, T., McMinn, A. and Suzuki, K. (2020) Differences in diversity and photoprotection capability between ice algae and under-ice phytoplankton in Saroma-Ko Lagoon, Japan: a comparative taxonomic diatom analysis with microscopy and DNA barcoding. *Polar Biology*, 43 (11): 1873–1885.